Coverage Control in Constant Flow Environments Based on a Mixed Energy-time Metric

Yu Ru and Sonia Martinez

Abstract— **In this paper, we study a multi-vehicle coverage control problem in constant flow environments while taking into account both energy consumption and traveling time. More specifically, the metric (called the mixed energy-time metric) is a weighted sum of the energy consumption and the traveling time for a vehicle to travel from one point to another in constant flows when using the minimum energy control, and the objective is to find vehicle locations that can minimize the expected mixed energy-time required for the set of vehicles to cover a region. We propose a refined gradient based control law of which the convergence is proved via Hybrid Systems Theory. Simulations show that the refined gradient based control can achieve similar performance as the exact gradient based control.**

I. Introduction

Deployment of a group of mobile vehicles to collectively cover a certain region has been studied extensively [1]–[4] (for a more comprehensive treatment, refer to Chapter 5 in [5]). The objective is usually to maximize/minimize a function related to the sensing performance (e.g., the work in [1], [3]) or the traveling time (e.g., the work in [2], [4]). The underlying vehicle models can be either holonomic (e.g., [1], [4]) or nonholonomic (e.g., [2], [3]). There is limited work on coverage control in river environments; for example, in [4], mobile vehicles cannot run against flow and the objective is to deploy them to maximize the total area reachable in a fixed amount of time. For nonurgent tasks, the energy consumption of mobile vehicles powered by batteries of limited capacity can be more critical compared with the traveling time. In [6], we study the minimum energy control for holonomic vehicles in constant flow environments and propose a minimum energy metric to assign regions of the environment to them (for details, refer to Proposition 1).

In this paper, we study a coverage control problem in river environments while taking into account both traveling time and energy consumption. This is motivated by the facts that mobile vehicles are usually powered by batteries of limited capacity and for certain relatively urgent tasks the traveling time also needs to be taken into account. Therefore, we introduce a mixed energy-time metric based on the minimum energy control for mobile vehicles in constant flows, to capture a compromise between traveling time and energy consumption. Our objective is to drive a group of vehicles to a vehicle location configuration that locally minimizes this metric. Since the mixed metric induces Voronoi partitions that might not be convex and are difficult to compute exactly, we introduce lower and upper approximations that can be refined to be arbitrarily close to the exact partition. We propose a refined gradient based control law and prove its convergence by formulating vehicle evolutions as a hybrid system and utilizing the Hybrid Invariance Principle [7]. In our algorithm, region refinement is produced when a condition that guarantees objective minimization is violated, similarly in spirit to the self-triggered strategy of [8] for the sporadic update of vehicles' locations. Thus, our approach could be combined with [8] and provides a general methodology to deal with general metrics for which Voronoi regions are hard to compute but which can be approximated with an arbitrary precision at the expense of higher computational costs. Simulations show that the refined gradient based control can achieve similar performance as the exact gradient based control.

This work was supported in part by NSF Award CNS-0930946. The authors are with Dept. of Mechanical and Aerospace Engineering at UC San Diego, {yuru2,soniamd}@ucsd.edu

II. Problem Formulation

The studied flow environment is described by a bounded two-dimensional region $D = \{(x\ y)^T \in \mathbb{R}^2 \mid 0 \leq x \leq L,\ |y| \leq \frac{W}{2}\}$, where $L > 0$ (or $W > 0$) is the length (or width) of the region. The velocity field is a mapping $v : D \to \mathbb{R}^2$ which maps $(x\ y)^T$ to $(B\ 0)^T$ with $B > 0$, i.e., the flow is only in the x direction.

A vehicle runs at speed $u = (u_x\ u_y)^T$, and then its dynamics can be described by

$$\frac{dx}{dt} = u_x + B\ ,\ \frac{dy}{dt} = u_y\ . \tag{1}$$

We assume that vehicles can run against the flow. To quantify the minimum energy required for a vehicle to move from one point to another in the region D among all possible controls, we recall a (pseudo)-metric (and its expression) as introduced in [6].

Definition 1 Given two points p^1 and p^2 in the flow environment D, the energy metric $J(p^1, p^2)$ is defined as $J(p^1, p^2) = \min \int_0^{t_f} u^T u dt$, where t_f is free, u satisfies Eq. (1), and $x(0) = x_{p^1}$ (i.e., the x coordinate of p^1), $y(0) = y_{p^1}$ (i.e., the y coordinate of p^1), $x(t_f) = x_{p^2},\ y(t_f) = y_{p^2}$.

Proposition 1 [6] Given p^1 and p^2 in D with the velocity field $v = (B\ 0)^T$, the minimum energy is $J(p^1, p^2) = 2B(d_{p^1p^2} + x_{p^1} - x_{p^2})$, and the optimal control is $u(t) = -\frac{1}{2}(C_1\ C_2)^T$ for $t \in [0, t_f]$, where $C_1 = 2B(1 + \frac{x_{p^1} - x_{p^2}}{d_{p^1p^2}})$, $C_2 = \frac{2B(y_{p^1} - y_{p^2})}{d_{p^1p^2}}$, and $t_f = \frac{d_{p^1p^2}}{B}$. ♢

Given a set of n vehicles $\{1, 2, ..., n\}$ with locations $P = \{p^1, p^2, ..., p^n\}$ and a task at $q \in D$, we are interested in assigning a vehicle from P to serve the task using *the minimum*

energy control. We do so using a multi-center function [5]. To capture the importance of the location q, we consider a continuous density function $\phi : D \to \mathbb{R}_{\geq 0}$. The larger the value $\phi(q)$, the more important the location q is. Analogously to [5], one can use $\mathcal{H}_1(P) = \int_D \min_{p^i \in P} J(p^i, q)\phi(q)dq$ to determine a locally optimal sensor configuration and region partition. At a local minimum, a task at q is assigned to p^i iff it can be reached with smaller energy from p^i than from any other p^j using the minimum-energy control of Proposition 1. Alternatively, let $t(p^i, q)$ be the traveling time from p^i to q along a straight line with velocity w (i.e., the *minimum-time control* with velocity w). Similarly to what has been done in multi-objective optimization, one could consider the mixed objective $\int_D \min_{p^i \in P}(\beta J(p^i, q) + (1-\beta)t(p^i, q))\phi(q)dq$ to balance between energy consumption and traveling time to serve q, where $\beta \in [0, 1]$. However, it is not clear how p^i should be controlled to reach an assigned q under this cost as the underlying control strategies (minimum energy/minimum time) are different — or how to find u with the mixed cost $\beta J(p^i, q) + (1-\beta)t(p^i, q)$.

Using exclusively the minimum-energy control, we can factor in a time cosideration in $\mathcal{H}_1$ as follows. For $\beta \in [0, 1]$, define:

$$J_{\text{mix}}(p^1, p^2) = \beta J(p^1, p^2) + (1-\beta)t_f \ . \tag{2}$$

Then $\min_{p^i \in P} J_{\text{mix}}(p^i, q)$ is the minimum mixed energy-time required for the set of vehicles to serve the task at q using the minimum-energy control. The expected minimum mixed energy-time for P to cover D is then given as:

$$\mathcal{H}(P) = \int_D \left(\min_{p^i \in P} J_{\text{mix}}(p^i, q) \right) \phi(q)dq \ . \tag{3}$$

Observe that, when $\beta = 0$, a locally optimal solution to $\mathcal{H}$ assigns q to p^i iff it can be reached with less time from p^i than from any other p^j but using the minimum-energy control. Other mixed metrics can be defined by choosing alternative motion control strategies (e.g., the minimum time control).

Now our coverage control problem is to find an algorithm that takes vehicles from their initial locations to local minima of $\mathcal{H}(P)$. The region assignment is given in terms of the following generalized Voronoi partition.

Definition 2 Let $P = \{p^1, p^2, ..., p^n\} \subset \mathbb{R}^2$ be a set of distinct points, where $n \geq 2$. We call the region given by

$$V(p^i) = \{p \in D \mid J_{\text{mix}}(p^i, p) \leq J_{\text{mix}}(p^j, p) \text{ for } j \neq i, j \in I_n\}$$

the mixed Voronoi cell associated with p^i, and the set given by $\mathcal{V} = \{V(p^1), V(p^2), ..., V(p^n)\}$ the mixed Voronoi partition generated by P, where $I_n := \{1, 2, ..., n\}$. Now, p^i and p^j for $i \neq j$ are Voronoi neighbors if $V(p^i) \cap V(p^j)$ is non-empty and non-trivial (i.e., not a single point). We use $\mathcal{N}_V(p^i)$ to denote the set of Voronoi neighbors of p^i.

Using the Voronoi partition just introduced, the function $\mathcal{H}(P)$ can be equivalently rewritten as

$$\mathcal{H}(P) = \sum_{i=1}^{n} \int_{V(p^i)} J_{\text{mix}}(p^i, q)\phi(q)dq \ . \tag{4}$$

Since the mixed energy-time metric induced Voronoi partition plays an important role in the algorithm design (refer to Section IV), we study such partition in the next section.

III. Mixed Voronoi Cells: Approximation

In this section, we first study the exact Voronoi cells, and then propose their lower and upper approximations.

A. Exact Voronoi Cells for Two Generators

By plugging in the expressions of $J(p^1, p^2)$ and t_f of Proposition 1 into Eq. (2), we obtain $J_{\text{mix}}(p^1, p^2) = A_1 d_{p^1 p^2} + A_2(x_{p^1} - x_{p^2})$, where $A_1 = 2B\beta + \frac{1-\beta}{B}$ and $A_2 = 2B\beta$. Since $\beta \in [0, 1]$, we have $0 \leq A_2 \leq A_1$, and $A_1 > 0$.

We study the Voronoi partition of two generators p^1, p^2. Following Definition 2, we have $V(p^1) = \{p \in D \mid J_{\text{mix}}(p^1, p) \leq J_{\text{mix}}(p^2, p)\}$. Based on the expression of $J_{\text{mix}}(p^i, p)$, $J_{\text{mix}}(p^1, p) \leq J_{\text{mix}}(p^2, p)$ is equivalent to

$$A_1 d_{p^1 p} + A_2(x_{p^1} - x_p) \leq A_1 d_{p^2 p} + A_2(x_{p^2} - x_p) \ ,$$
$$d_{p^1 p} - d_{p^2 p} \leq \frac{A_2}{A_1}(x_{p^2} - x_{p^1}) \ . \tag{5}$$

Now we have $V(p^1) = \{p \in D \mid d_{p^1 p} - d_{p^2 p} \leq \frac{A_2}{A_1}(x_{p^2} - x_{p^1})\}$, and the boundary between p^1 and p^2 is any $p \in D$ that satisfies $d_{p^1 p} - d_{p^2 p} = \frac{A_2}{A_1}(x_{p^2} - x_{p^1})$.

Without loss of generality, we assume that $x_{p^1} < x_{p^2}$ and $y_{p^1} < y_{p^2}$. If $\beta = 0$, then $A_2 = 0$. The Voronoi cell boundary is the perpendicular bisector of $p^1 p^2$, and the Voronoi cells are polygons. In the following, we assume that $0 < \beta \leq 1$.

For any point p on the boundary, we have $d_{p^1 p} - d_{p^2 p} = \frac{A_2}{A_1}(x_{p^2} - x_{p^1}) > 0$, which defines a hyperbolic curve. To derive its equation, we first transform the coordinate from $x - y$ plane to $x' - y'$ plane such that the origin is at $(\frac{x_{p^1} + x_{p^2}}{2} \ \frac{y_{p^1} + y_{p^2}}{2})^T$ and the positive x' direction is from p^1 to p^2. Any point p with coordinates $(x_p \ y_p)^T$, has new coordinates

$$x'_p = (x_p - \tfrac{x_{p^1} + x_{p^2}}{2}) \cos\alpha + (y_p - \tfrac{y_{p^1} + y_{p^2}}{2}) \sin\alpha \ , \tag{6}$$
$$y'_p = -(x_p - \tfrac{x_{p^1} + x_{p^2}}{2}) \sin\alpha + (y_p - \tfrac{y_{p^1} + y_{p^2}}{2}) \cos\alpha \ , \tag{7}$$

where α satisfies $\tan\alpha = \frac{y_{p^2} - y_{p^1}}{x_{p^2} - x_{p^1}}$ and is shown in Fig. 1(a). The boundary is shown in Fig. 1(b) as the red dashed line in the $x' - y'$ plane, and can be described by the equation $\frac{(x'_p)^2}{a^2} - \frac{(y'_p)^2}{b^2} = 1$, where $a = \frac{(x_{p^2} - x_{p^1})A_2}{2A_1}$, $c = \frac{d_{p^1 p^2}}{2}$, $b = \sqrt{c^2 - a^2}$, and $x'_p \geq a$. The coordinates for p^* in Fig. 1(b) (namely, the intersection point between the boundary and the x' axis) are $(a \ 0)^T$. The transformation given by Eqs. (6) and (7) can be used to obtain the expression of the boundary in the $x - y$ plane. Similarly, we can derive boundary equations for the cases with $x_{p^1} \geq x_{p^2}$ and/or $y_{p^1} \geq y_{p^2}$.

It can be verified that $V(p^1)$ is not convex. In general, the Voronoi partition of n generators will contain non-convex regions. Calculating the exact $V(p^i)$, for $i \in I_n$, is challenging because the cell boundary consists of pieces of hyperbolas, which requires solving 4th order equations in general. Instead, we will study approximations of Voronoi cells in the next subsection.

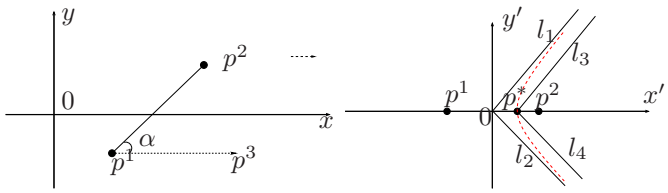

(a) Original coordinates. (b) Transformed coordinates.

Fig. 1. Voronoi partition generated by $\{p^1, p^2\}$ satisfying $x_{p^1} < x_{p^2}$ and $y_{p^1} < y_{p^2}$. The red dashed line is the boundary.

B. Voronoi Cells for Two Generators: Approximations

In this subsection, we present lower and upper approximations of Voronoi cells through hyperbola asymptotes, along the lines of [6] (only the case $\beta = 1$ is considered in [6]). Here, we focus on two points p^1 and p^2 satisfying $x_{p^1} < x_{p^2}$ and $y_{p^1} < y_{p^2}$. In the $x' - y'$ plane of Fig. 1(b), the equation for l_1 (or l_2) is $y' = \frac{b}{a}x'$ (or $y' = -\frac{b}{a}x'$), where $a = \frac{(x_{p^2} - x_{p^1})A_2}{2A_1}$ and $b = \sqrt{c^2 - a^2}$. It can be verified that

$$D'_{\text{lower}}(p^1|p^2) = \{(x'\ y')^T \in D' \mid x' \le \tfrac{a}{b}y' \text{ if } y' \ge 0, x' \le -\tfrac{a}{b}y' \text{ if } y' < 0\} \ ,$$

i.e., the lower approximation of $V'(p^1)$ given p^2, satisfies $D'_{\text{lower}}(p^1|p^2) \subseteq V'(p^1)$, where $D'_{\text{lower}}(p^1|p^2)$ (or $V'(p^1)$) is the region $D_{\text{lower}}(p^1|p^2)$ (or the Voronoi cell $V(p^1)$) in the transformed $x' - y'$ plane. Going back to the $x - y$ plane, we have $D_{\text{lower}}(p^1|p^2) \subseteq V(p^1)$. Similarly, $V(p^2) \subseteq D_{\text{upper}}(p^2|p^1) = D \setminus D_{\text{lower}}(p^1|p^2)$.

To obtain an upper approximation for $V(p^1)$, we use l_3 (which is parallel to l_1) and l_4 (which is parallel to l_2) passing through p^* in Fig. 1(b). The equation for l_3 (or l_4) is $y' = \frac{b}{a}(x' - a)$ (or $y' = -\frac{b}{a}(x' - a)$). It can be verified that

$$D'_{\text{upper}}(p^1|p^2) = \{(x'\ y')^T \in D' \mid x' \le \tfrac{a}{b}y' + a \text{ if } y' \ge 0, x' \le -\tfrac{a}{b}y' + a \text{ if } y' < 0\}$$

satisfies $V'(p^1) \subseteq D'_{\text{upper}}(p^1|p^2)$. Going back to the $x - y$ plane, we have $V(p^1) \subseteq D_{\text{upper}}(p^1|p^2)$. Similarly, we obtain $D_{\text{lower}}(p^2|p^1) = D \setminus D_{\text{upper}}(p^1|p^2)$ for $V(p^2)$.

Since $l_1, \ldots, l_4$ play an important role in the approximations, we present their equations in the $x - y$ plane. For l_1, we have $y' = \frac{b}{a}x'$. Using Eqs. (6) and (7), we obtain:

$$y - \tfrac{y_{p^1} + y_{p^2}}{2} = (x - \tfrac{x_{p^1} + x_{p^2}}{2}) \times \frac{A_2 \sin\alpha + \cos\alpha\sqrt{A_1^2 \sec\alpha^2 - A_2^2}}{A_2 \cos\alpha - \sin\alpha\sqrt{A_1^2 \sec\alpha^2 - A_2^2}} \ . \quad (8)$$

For l_2, $y' = -\frac{b}{a}x'$. Using Eqs. (6) and (7), we obtain:

$$y - \tfrac{y_{p^1} + y_{p^2}}{2} = (x - \tfrac{x_{p^1} + x_{p^2}}{2}) \times \frac{A_2 \sin\alpha - \cos\alpha\sqrt{A_1^2 \sec\alpha^2 - A_2^2}}{A_2 \cos\alpha + \sin\alpha\sqrt{A_1^2 \sec\alpha^2 - A_2^2}} \ . \quad (9)$$

Since l_3 (or l_4) is parallel to l_1 (or l_2) and passes through $p^* = p^1 + \frac{c+a}{2c}(p^2 - p^1)$, we can similarly obtain its equation in the $x - y$ plane. The asymptote equations for $x_{p^1} \ge x_{p^2}$ and/or $y_{p^1} \ge y_{p^2}$ can be readily obtained.

When we calculate the control in Section IV, the calculation will depend on integrals over Voronoi cells. Since the exact Voronoi cells are difficult to obtain, we will use lower and upper approximations instead. To reduce the error in control actions, we need a procedure to refine the approximations. Suppose we have obtained lower approximations for p^1 and p^2 as in Fig. 2. That is, $V(p^1)$ is lower approximated by $D_{\text{lower}}(p^1|p^2)$ (i.e., the polygon $p_1p_6p_7p_{11}p_{10}p_4$),

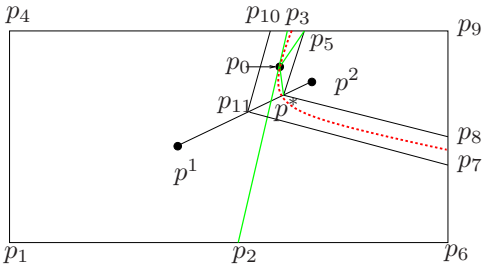

Fig. 2. Refined Voronoi cells.

and $V(p^2)$ is lower approximated by $D_{\text{lower}}(p^2|p^1)$ (i.e., the polygon $p_8p_9p_5p^*$). Select one point on the Voronoi boundary inside D (such as p_0 in Fig. 2), then draw a tangent line of the boundary at p_0, which intersects with the environment boundary at p_2, p_3. The union of the polygons $p_1p_6p_7p_{11}p_{10}p_4$ and $p_1p_2p_3p_4$ is a better lower approximation of $V(p^1)$. For $V(p^2)$, we can form the triangle $p^*p_0p_5$, and then take the union of the polygon $p_8p_9p_5p^*$ with the triangle $p^*p_0p_5$, which is a better lower approximation of $V(p^2)$. Repeating the above procedure by adding more distinct points like p_0, the refined approximation $D^{\text{refined}}_{\text{lower}}(p^1|p^2)$ (or $D^{\text{refined}}_{\text{lower}}(p^2|p^1)$) can be made arbitrarily close to $V(p^1)$ (or $V(p^2)$). At the same time, we also get refined upper approximations $D^{\text{refined}}_{\text{upper}}(p^1|p^2) = D \setminus D^{\text{refined}}_{\text{lower}}(p^2|p^1)$ and $D^{\text{refined}}_{\text{upper}}(p^2|p^1) = D \setminus D^{\text{refined}}_{\text{lower}}(p^1|p^2)$.

C. Voronoi Cells for Multiple Generators: Approximations

The idea of refined approximations can be generalized to multiple generators using the concept of Voronoi neighbors in Definition 2. In general, if there are n points, we can get the lower and upper approximations of $V(p^i)$ using

$$V_{\text{lower}}(p^i) = \cap_{p^j \in \mathcal{N}_V(p^i)} D_{\text{lower}}(p^i|p^j) \ , \quad (10)$$

$$V_{\text{upper}}(p^i) = \cap_{p^j \in \mathcal{N}_V(p^i)} D_{\text{upper}}(p^i|p^j) \ , \quad (11)$$

and the refined lower and upper approximations using

$$V^{\text{refined}}_{\text{lower}}(p^i) = \cap_{p^j \in \mathcal{N}_V(p^i)} D^{\text{refined}}_{\text{lower}}(p^i|p^j) \ , \quad (12)$$

$$V^{\text{refined}}_{\text{upper}}(p^i) = \cap_{p^j \in \mathcal{N}_V(p^i)} D^{\text{refined}}_{\text{upper}}(p^i|p^j) \ . \quad (13)$$

The regions $V^{\text{refined}}_{\text{upper}}(p^i)$ and $V^{\text{refined}}_{\text{lower}}(p^i)$ can be made arbitrarily close to $V(p^i)$ using the procedure in the previous subsection.

IV. Motion Coordinated Control

In this section, we propose a gradient-based control law calculated using the lower approximation of Voronoi cells, and study its convergence property.

A. Approximate Gradient Based Control

To find P that (locally) minimizes $\mathcal{H}(P)$ in Eq. (4), we use a gradient based control. More specifically, we take the partial derivative of $\mathcal{H}$ with respect to each point p^i, and obtain

$$\frac{\partial \mathcal{H}}{\partial p^i} = \int_{V(p^i)} \left(A_1 \frac{p^i - q}{\|pi - q\|} + A_2 \begin{bmatrix} 1 \\ 0 \end{bmatrix} \right) \phi(q) dq \ , \quad (14)$$

which is derived based on Theorem 2.16 in [5]. We implement the gradient based control policy by setting $U =$

$-\frac{\partial \mathcal{H}}{\partial p^i} - (B\ 0)^T$. Therefore, the closed loop system for the vehicle i is $\frac{dp^i}{dt} = -\frac{\partial \mathcal{H}}{\partial p^i}$.

Note that to calculate the control law, we need compute the gradient, which involves the calculation of the integral over Voronoi cells. Since it is difficult (if not impossible) to obtain the exact Voronoi cells, we use the refined lower approximation $V_{\text{lower}}^{\text{refined}}(p^i)$ in Eq. (12) to calculate the approximated gradient as

$$\frac{\partial \mathcal{H}}{\partial p^i}\Big|_x^{\text{approx}} = \int_{V_{\text{lower}}^{\text{refined}}(p^i)} \left(A_1 \frac{x_{p^i} - x_q}{\|pi - q\|} + A_2\right) \phi(q) dq \ , \quad (15)$$

$$\frac{\partial \mathcal{H}}{\partial p^i}\Big|_y^{\text{approx}} = \int_{V_{\text{lower}}^{\text{refined}}(p^i)} A_1 \frac{y_{p^i} - y_q}{\|pi - q\|} \phi(q) dq \ . \quad (16)$$

Now the control U is given as $U = -\frac{\partial \mathcal{H}}{\partial p^i}|^{\text{approx}} - (B\ 0)^T$, and the closed loop system for the vehicle i is

$$\frac{dp^i}{dt} = -\frac{\partial \mathcal{H}}{\partial p^i}|^{\text{approx}} \ . \quad (17)$$

If the true gradient in Eq. (14) is used, it can be verified (by a proof similar to the one to Theorem 5.5 in [5]) that the vehicles will converge to a set of locations that locally minimize the function $H(P)$. However, this is not necessarily the case when the approximated gradient is utilized. In the following theorem, we show that under certain condition on the approximated gradient, the control based on the approximated gradient in Eqs. (15) and (16) will strictly decrease the function $\mathcal{H}(P)$.

Theorem 1 Given the closed loop dynamics for vehicle i in Eq. (17), for $i \in I_n$:

(i) Suppose that, for every vehicle i and any time t,

$$G_i \times S_i(t) < \|K_i(t)\| \ , \quad (18)$$

whenever $\|K_i(t)\| > 0$, where $K_i(t) = \frac{\partial \mathcal{H}}{\partial p^i}|^{\text{approx}}(t)$, $G_i = \sup_{p^i \in D, q \in D} \|\frac{\partial J_{\text{mix}}(p^i, q)}{\partial p^i} \phi(q)\|$, and $S_i(t) = \text{area}(V_{\text{upper}}^{\text{refined}}(p^i(t)) \setminus V_{\text{lower}}^{\text{refined}}(p^i(t)))$. Now, if there is at least one i for which $\|K_i(t)\| > 0$ holds, then $\frac{d\mathcal{H}(P)}{dt} < 0$.

(ii) Suppose that, for every vehicle i and any time t, Eq. (18) is satisfied whenever $\|K_i(t)\| > 0$. Then $\frac{d\mathcal{H}(P)}{dt} = 0$ if and only if for every vehicle i, $\frac{\partial \mathcal{H}}{\partial p^i}|^{\text{approx}} = (0\ 0)^T$ (or equivalently, $\|\frac{\partial \mathcal{H}}{\partial p^i}|^{\text{approx}}\| = 0$).

Proof: Part (i). It can be verified that

$$\frac{d\mathcal{H}(P)}{dt} = \sum_{i=1}^{n} \frac{\partial \mathcal{H}}{\partial p^i} \cdot \frac{dp^i}{dt} = -\sum_{i=1}^{n} J_i \cdot K_i \ , \quad (19)$$

where $\cdot$ is the dot product, $J_i = \frac{\partial \mathcal{H}}{\partial p^i}$, and $K_i = \frac{\partial \mathcal{H}}{\partial p^i}|^{\text{approx}}$. Therefore, for vehicle i satisfying $\|K_i\| = 0$, it does not contribute to $\frac{d\mathcal{H}(P)}{dt}$. We can show $\frac{d\mathcal{H}(P)}{dt} < 0$ as long as $J_i \cdot K_i > 0$ for every i satisfying $\|K_i\| > 0$. We first bound $\|J_i - K_i\|$ as below.

$$\begin{aligned}\|J_i - K_i\| &= \|\int_{V(p^i) \setminus V_{\text{lower}}^{\text{refined}}(p^i)} \frac{\partial J_{\text{mix}}(p^i, q)}{\partial p^i} \phi(q) dq\| \\ &\le \sup_{p^i \in D, q \in D} \|\frac{\partial J_{\text{mix}}(p^i, q)}{\partial p^i} \phi(q)\| \times \\ &\quad \|\int_{V(p^i) \setminus V_{\text{lower}}^{\text{refined}}(p^i)} 1 dq\| \\ &\le G_i \times S_i \ .\end{aligned}$$

If $G_i \times S_i < \|K_i\|$ as in Eq. (18), we have $|\|J_i\| - \|K_i\|| \le \|J_i - K_i\| \le G_i \times S_i < \|K_i\|$, which implies that

$$0 < \|K_i\| - G_i \times S_i \le \|J_i\| \le \|K_i\| + G_i \times S_i \ . \quad (20)$$

Now we can check $J_i \cdot K_i$. It can be verified that $J_i \cdot K_i = \frac{\|J_i\|^2 + \|K_i\|^2 - \|J_i - K_i\|^2}{2}$. Therefore,

$$\begin{aligned}J_i \cdot K_i &\ge \frac{(\|K_i\| - G_i \times S_i)^2 + \|K_i\|^2 - (G_i \times S_i)^2}{2} \\ &= \|K_i\|(\|K_i\| - G_i \times S_i) \ . \quad (21)\end{aligned}$$

Since $0 \le G_i \times S_i(t) < \|K_i\|$, $J_i \cdot K_i > 0$.

Therefore, if there is at least one i for which $\|K_i(t)\| > 0$, then $\frac{d\mathcal{H}(P)}{dt} < 0$.

Part (ii). The if part is straightforward since $\frac{d\mathcal{H}(P)}{dt} = -\sum_{i=1}^{n} J_i \cdot K_i$ where $K_i = \frac{\partial \mathcal{H}}{\partial p^i}|^{\text{approx}}$. Now we prove the only if part. During the evolution of vehicle i, since Eq. (18) is satisfied if $\|\frac{\partial \mathcal{H}}{\partial p^i}|^{\text{approx}}(t)\| > 0$, then $\|K_i\|(\|K_i\| - G_i \times S_i) \ge 0$ always holds. By combining Eqs. (19) and (21), we have $\frac{d\mathcal{H}(P)}{dt} = -\sum_{i=1}^{n} J_i \cdot K_i \le -\sum_{i=1}^{n} \|K_i\|(\|K_i\| - G_i \times S_i) \le 0$. If $\frac{d\mathcal{H}(P)}{dt} = 0$, then we must have $\|K_i\|(\|K_i\| - G_i \times S_i) = 0$ for every vehicle i. If $\|K_i\| > 0$, we have $G_i \times S_i < \|K_i\|$, which implies that $\|K_i\|(\|K_i\| - G_i \times S_i) > 0$. Therefore, the only possibility is that $\|K_i\| = 0$ for every vehicle i, i.e., $\frac{\partial \mathcal{H}}{\partial p^i}|^{\text{approx}} = (0\ 0)^T$ for every vehicle i. ■

Since $G_i \le \sqrt{A_1^2 + (A_1 + A_2)^2} \sup_{q \in D} \phi(q)$, S_i and $\|\frac{\partial \mathcal{H}}{\partial p^i}|^{\text{approx}}\|$ can be calculated (because the approximated Voronoi cells are polygons), the condition in Eq. (18) can be checked. If the condition is violated, we can refine the lower and upper approximations so that it holds again as long as $\|\frac{\partial \mathcal{H}}{\partial p^i}|^{\text{approx}}(t)\| > 0$. The importance of Theorem 1 is that as long as the condition in Eq. (18) holds for every vehicle, the control policy based on the approximated gradient strictly decreases the value of the function $\mathcal{H}$ until the approximated gradient for every vehicle becomes zero.

Now the basic idea of seeking P to minimize $\mathcal{H}(P)$ is the following: for each vehicle i, it starts at a location $p^i(0) \in D$; and then follows the closed loop dynamic in Eq. (17) while guaranteeing that, if $\|\frac{\partial \mathcal{H}}{\partial p^i}|^{\text{approx}}(t)\| > 0$ but Eq. (18) does not hold, then it refines its own approximated Voronoi cell until Eq. (18) holds again. The detailed algorithm is given in Algorithm 1. In the algorithm, we introduce prescribed $\epsilon > \bar{\epsilon} > 0$ so that i) if $\|K_i(t)\| < \epsilon$, $U(t) = -(B\ 0)^T$, ii) if $\|K_i(t)\| \ge \epsilon$ and $G_i \times S_i(t) + \bar{\epsilon} \ge \|K_i(t)\|$ (which implies that the condition in Eq. (18) is violated since $\bar{\epsilon}$ can be arbitrarily small), then the approximated Voronoi cells are

Algorithm 1 Coverage Control Algorithm

Input: The region D, B, β, $\phi(q)$ for $q \in D$, initial locations of all vehicles $\{p^1(t_0), p^2(t_0), ..., p^n(t_0)\}$, infinitely small δt, and prescribed $\epsilon > \bar{\epsilon} > 0$

Output: Continuous control actions $U(t)$

Each vehicle $i \in \{1, 2, ..., n\}$ performs the following actions:

1: Initialize $A_1 = 2B\beta + \frac{1-\beta}{B}$ and $A_2 = 2B\beta$;
2: Set $G_i = \sqrt{A_1^2 + (A_1 + A_2)^2}\sup_{q\in D}\phi(q)$;
3: Initialize $t = t_0$;
4: Compute the approximations $V_{\text{lower}}(p^i)$ and $V_{\text{upper}}(p^i)$ using Eqs. (10) and (11);
5: Calculate $K_i(t) = \frac{\partial \mathcal{H}}{\partial p^i}|^{\text{approx}}(t)$, and $S_i(t) = \text{area}(V_{\text{upper}}(p^i(t)) \setminus V_{\text{lower}}(p^i(t)))$;
6: **if** $\|K_i(t)\| \geq \epsilon$ **then**
7: **if** $G_i \times S_i(t) + \bar{\epsilon} \geq \|K_i(t)\|$ **then**
8: Refine the lower and upper approximations of $V(p^i)$ using the procedure in Section III-B and Eqs. (12), (13) until the updated $K_i'(t)$ and $S_i'(t)$ satisfy either a) $G_i \times S_i'(t) + \bar{\epsilon} \leq \|K_i'(t)\|$ or b) $\|K_i'(t)\| \leq \epsilon$;
9: Set $U(t) = -K_i'(t) - (B\ 0)^T$ if a) holds, and $U(t) = -(B\ 0)^T$ otherwise;
10: **else**
11: Set $U(t) = -K_i(t) - (B\ 0)^T$;
12: **end if**
13: **else**
14: Set $U(t) = -(B\ 0)^T$;
15: **end if**
16: Apply $U(t)$ between t and $t + \delta t$;
17: Update t with $t + \delta t$ and go to Step 4;

refined and appropriate controls are calculated based on the updated $K_i'(t)$ and $S_i'(t)$ (refer to Step 8 in the algorithm). The introduction of ϵ and $\bar{\epsilon}$ is for the sake of convergence proof (and also leads to implementations that are more robust to finite numerical precision). One assumption we made is that each vehicle has continuous access to the locations of its Voronoi neighbors.

B. Convergence

In this subsection, we show that the refined gradient based control converges.

Theorem 2 Given the optimization problem $\mathcal{H}(P)$ in Eq. (4), for any $\epsilon > \bar{\epsilon} > 0$ and any initial vehicle locations in D, vehicles following the refined gradient based control in Algorithm 1 asymptotically converge to the set $\{P = \{p^1, ..., p^n\}, p^i \in D \mid |\frac{dH(P)}{dt}| \leq \epsilon M n\}$, where $M = \sup\|\frac{\partial H}{\partial p^i}\| < \infty$ and n is the number of vehicles.

Proof: The proof is based on formulating the evolution of Algorithm 1 as a hybrid system and utilizing the Hybrid Invariance Principle [7]. For details, refer to [9]. ■

Remark 1 If $\beta = 0$, then $J_{\text{mix}}(p^1, p^2) = t_f = \frac{d_{p^1p^2}}{B}$, which is essentially the Euclidean distance metric. Therefore, the Voronoi partition is the standard Voronoi partition. In this case, the upper and lower approximations proposed in Section III-C coincide with the exact Voronoi cells, which implies that $S_i = 0$. Therefore, the condition in Eq. (18) is always true as long as $\|\frac{\partial \mathcal{H}}{\partial p^i}\| \neq 0$. In other words, the gradient based control is always minimizing the function $\mathcal{H}(P)$ for the Euclidean distance metric until $\|\frac{\partial \mathcal{H}}{\partial p^i}\| = 0$ for every i, which is consistent with existing results. ♢

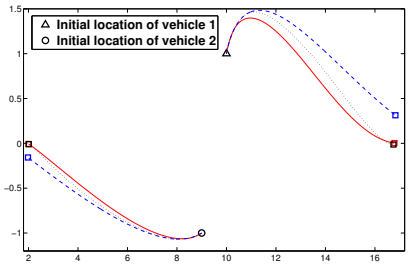

Fig. 3. Trajectories of vehicles 1 and 2 with the exact gradient based control (the solid red curve), the refined gradient based control (the dotted black curve), and the approximate gradient based control (the dashed blue curve).

V. Simulations

For the studied region D, we set $L = 30$, $W = 10$. For simplicity, we use $B = 1$ for the flow, and $\beta = 0.5$ in the mixed energy-time metric, $\phi(q) = 1$ for the density, and δt in Algorithm 1 is chosen to be 0.01. We first focus on two vehicles, i.e., vehicle 1 with initial location $(10\ 1)^T$ and vehicle 2 with initial location $(9\ -1)^T$. In this case, the exact Voronoi cell as well as the exact gradient can be calculated; therefore, we can compare the performance of the control based on the approximate gradient and the exact gradient. When the gradient is calculated based on the exact Voronoi cell (or the refined lower approximation in Eq. (12) while guaranteeing that the condition in Eq. (18) holds, or the lower approximation in Eq. (10), respectively), correspondingly the control is referred to as the exact gradient based control (or the refined gradient based control, or the approximate gradient based control, respectively), and the trajectories[1] for vehicles 1 and 2 are plotted in Fig. 3 using the solid red curves (or the dotted black curves, or the dashed blue curves, respectively). It can be observed that for vehicle 1, the trajectory using the exact gradient based control is slightly different from the trajectory using the refined gradient based control but the final locations in both case are very close. In contrast, not only the trajectory but also the final location using the exact gradient based control are very different from those using the approximate gradient based control. Similar observations also hold for vehicle 2 but the differences are smaller.

When comparing the evolutions[2] of $\mathcal{H}(P)$ using three different controls, they are very close as shown in Fig. 4(a).

[1]Note that the simulation duration is chosen to be around 7. This is because for the refined gradient based control, after 7 the refined gradient is close to zero and the condition in Eq. (18) can hardly be satisfied even after repeated refinement of the approximations.

[2]In general, the cost $\mathcal{H}(P)$ can be calculated based on Eq. (3). For two generators, since the exact Voronoi cell can be obtained, the cost can also be calculated based on Eq. (4).

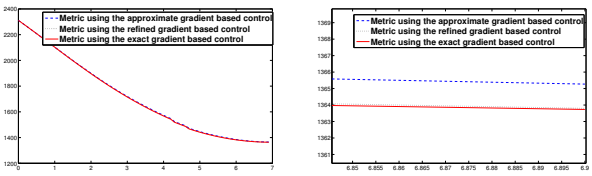

(a) Evolution of the cost function.

(b) Enlarged portion of the cost function.

Fig. 4. The evolution of $\mathcal{H}(P)$ using the exact gradient based control (the solid red curve), the refined gradient based control (the dotted black curve), and the approximate gradient based control (the dashed blue curve).

A closer look at the cost at the end of the simulations, the costs using the exact gradient based control and the refined gradient based control are almost indistinguishable, and they are slightly lower than the cost using the approximate gradient based control (similar results are observed for more simulations). Note that the slight reduction in the cost (more accurately, the relative percentage of cost reduction is 0.15%) is at the expense of tremendous efforts that are necessary to calculate the exact gradient and the refined gradient. For more than two generators, it is very difficult to calculate the exact gradient (due to the difficulty of calculating the intersection of multiple hyperbolas) and the refined gradient (because the Matlab built-in procedure for calculating the unions of polygons is not reliable, and the unions of polygons are needed when refining the approximations as explained in Section III-B). Therefore, we will only use the approximate gradient based control in the following simulation.

We now examine seven vehicles, of which the initial locations are denoted using the circle marker in Fig. 5(a). Using the approximate gradient based control, the trajectories of the seven vehicles are shown in Fig. 5(a) with the square marker denoting the final locations and the polygons denoting the approximated Voronoi cells; the evolution of the cost function is plotted in Fig. 5(b). One interesting observation is that the approximate gradient based control may occasionally increase the cost slightly and then decrease it again; this might be because for this control, the condition in Eq. (18) is not guaranteed. However, the vehicles do converge to a fixed configuration. This is also observed by more extensive simulations; the results are not illustrated due to the limited space.

VI. Conclusions

In this paper, we studied a multi-vehicle coverage control problem in constant flow environments while taking into account both the energy consumption and the traveling time. We proposed a gradient based control law which is calculated based on the refined approximated Voronoi cells and proved its convergence using the Hybrid Invariance Principle. Simulations show that the refined gradient based control can achieve similar performance as the exact gradient based control.

In this work, we assume that each vehicle has continuous access to the locations of its Voronoi neighbors. We are looking into radius adjusting algorithms (that generalize the algorithm in Table 1 of [1] for standard Voronoi partitions)

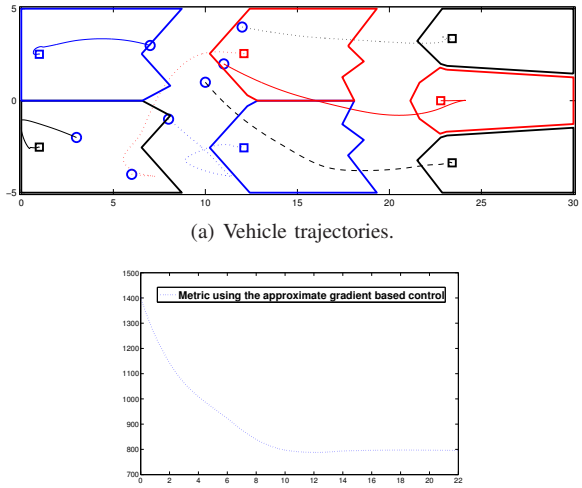

(a) Vehicle trajectories.

(b) Evolution of the cost.

Fig. 5. Trajectories of seven vehicles and the corresponding evolution of the cost function using the approximate gradient based control.

to enable a vehicle to calculate its approximated Voronoi cell more efficiently. In addition, we plan to explore the self-triggered idea in [8] to enable a vehicle to request other vehicle's locations only when a certain condition holds (instead of continuous requests). In terms of generalizing the current work, possible directions could be i) exploring more complicated agents' dynamics and extending the introduced metric, ii) bounding the lower approximation and its effects on the convergence of the refined gradient based control, iii) examining the convergence of the approximate gradient based control though simulations show that it always converges, and iv) investigating the possibility of agents' collision when running the algorithms, and more efficient ways to refine approximated Voronoi cells.

References

[1] J. Cortés, S. Martinez, T. Karatas, and F. Bullo, "Coverage control for mobile sensing networks," *IEEE Transactions on Robotics and Automation*, vol. 20, pp. 243–255, Apr. 2004.

[2] J. Enright, K. Savla, and E. Frazzoli, "Coverage control for nonholonomic agents," in *Proc. of the 47th IEEE Conf. on Decision and Control*, 2008, pp. 4250–4256.

[3] J.-M. Luna, R. Fierro, C. Abdallah, and J. Wood, "An adaptive coverage control algorithm for deployment of nonholonomic mobile sensors," in *Proc. of the 49th IEEE Conf. on Decision and Control*, Dec. 2010, pp. 1250–1256.

[4] A. Kwok and S. Martinez, "A coverage algorithm for drifters in a river environment," in *Proc. of the American Control Conference*, 2010, pp. 6436–6441.

[5] F. Bullo, J. Cortes, and S. Martinez, *Distributed Control of Robotic Networks: A Mathematical Approach to Motion Coordination Algorithms*. Princeton University Press, 2009.

[6] Y. Ru and S. Martinez, "Energy-based Voronoi partition in constant flow environments," submitted to *IEEE Transactions on Automation Science and Engineering*, 2011. [Online]. Available: http://arxiv.org/abs/1111.0071

[7] R. Sanfelice, R. Goebel, and A. Teel, "Results on convergence in hybrid systems via detectability and an invariance principle," in *Proc. of American Control Conference*, 2005, pp. 551–556.

[8] C. Nowzari and J. Cortés, "Self-triggered coordination of robotic networks for optimal deployment," in *Proc. of American Control Conference*, San Francisco, 2011, pp. 1039–1044.

[9] Y. Ru and S. Martinez, "Coverage control in constant flow environments based on a mixed energy-time metric," submitted to *Automatica*, 2012.